

# High-order sideband generation of transient lasing without population inversion

Luqi Yuan<sup>1,\*</sup>, Da-Wei Wang<sup>1</sup>, Anatoly A. Svidzinsky<sup>1</sup>, and Marlan O. Scully<sup>1,2,3</sup>

<sup>1</sup>*Texas A&M University, College Station TX 77843;*

<sup>2</sup>*Princeton University, Princeton, NJ 08544;*

<sup>3</sup>*Baylor University, Waco, TX 76798*

\*Corresponding author: yuanluqi@gmail.com

(Dated: June 7, 2019)

We study high-order sideband generation of coherent short pulse emission without population inversion in the transient regime. We use a universal method to study the propagation of a pulse in various spectral regions through the gas medium strongly driven on a low-frequency transition on a time scale shorter than the decoherence time. The results show that gain on the high-order sidebands can be produced even if there is no initial population inversion prepared. This method has the potential to make high frequency lasers (such as in the extreme ultraviolet and x-ray spectral regions).

PACS numbers: 42.62.-b, 42.50.Gy

Lasing without inversion (LWI) [1–4] has been studied in various media, such as in gas [5], circuit quantum electrodynamics [6], and terahertz intersubband-based devices [7]. By preparing an atomic system in a coherent superposition of states it is possible to create atomic coherence to suppress absorption resulting in LWI [8]. One of the major goals in the field of LWI is to make table-top short wavelength laser pulses (such as the extreme ultraviolet (XUV) and x-ray) where it is difficult to prepare population inversion. However, the well-studied steady-state LWI requires that the decay rate of the incoherent pumped transition is larger than the one of the lasing transition [9], which is difficult to achieve when the frequency of the lasing transition is higher than the drive field frequency. In addition, the atomic levels for a conventional X-ray laser usually require a plasma which have rapid collisional and decoherence rates [10], which will destroy the coherence necessary for LWI. Fortunately, these obstacles can be overcome by transient LWI [4], where the lasing happens at a much shorter time than the decoherence time and therefore the decoherence can be neglected. A recent experiment in Helium plasma shows a collective atomic coherent effect on a time scale much shorter than the plasma collisional time [11]. This paves the way for more complicated manipulation of atomic coherence in LWI to achieve sideband lasing with even higher frequencies.

High-order sideband generation has wide applications in terahertz quantum cascade lasers [12], ultrafast driven optomechanical systems [13], polymer waveguides on a printed circuit [14], and so on [15, 16]. However, it needs coherent pumping fields which are rare in X-ray and XUV regime. In this letter, we combine the transient LWI and sideband generation to study high-order sideband LWI in a long atomic medium driven by a low-frequency field. The blue-shifted sidebands are promising for short-wavelength coherent light sources. We use a pencil-like medium for a mirrorless superradiant source

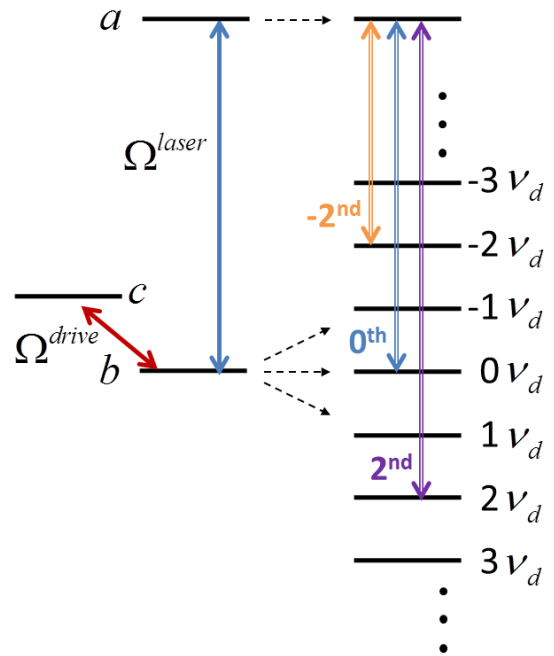


FIG. 1: (Color online) Left: Energy diagram for V-scheme; Right: Floquet ladder of states produced by the  $c \rightarrow b$  transition driven by a laser field with frequency  $\nu_d$ . Possible lasing transitions are the 0<sup>th</sup>-order transition ( $\sim \omega_{ab}$ ), and at the even sidebands  $\pm 2^{\text{nd}}$ -order ( $\sim \omega_{ab} \pm 2\nu_d$ ), etc.

with the ringing effect (energy oscillation between the medium and the field) [17]. The superradiant atomic coherence builds up in a time scale much shorter than all decoherence times [18]. The sidebands are generated by high order collective atomic coherence induced by a monochromatic driving field [19, 20]. In this process, counter-rotating terms play an equally important role as the rotating terms.

The mechanism of our proposal is shown in Fig. 1 (Left) based on a three-level V-type system. The system is initially prepared such that most of the popu-

lation remains in the ground state but a little population is in the excited state  $|a\rangle$ . This can be done either by an incoherent pump, which is turned off at time  $t = 0$ , or by non-radiative three-body recombination following an optical field ionization [11]. Then a strong driving field  $\Omega^{\text{drive}}$  propagates into the pencil-like active medium and couples the transition  $c \leftrightarrow b$  and generates a Floquet ladder [21] in the dressed state picture (see Fig. 1 (Right)). The transitions from  $a$  to the Floquet ladder produce various lasing fields with frequency  $\nu_l \sim \omega_{ab} \pm 2n\nu_d$  ( $n = 1, 2, 3, \dots$ ) in a time scale much shorter than any decay time. Here  $\nu_l$  is the lasing frequency,  $\omega_{ab}$  is the atomic transition,  $\nu_d$  is the driving field frequency. These fields are coupled by  $\Omega^{\text{drive}}$  via the atomic coherence. The frequency difference between sidebands is always an even multiple of  $\nu_d$  since an atom in state  $|i\rangle$  needs an even number of photons to return to its original state  $|i\rangle$ , through successive real and virtual processes (where the counter-rotating terms play a role) [22]. Although there is no population inversion in the bare basis, there may be inversion between the dressed state levels. For these inverted dressed states the corresponding lasing mode is amplified, and through the coupled atomic coherence, other larger sideband modes are consequently amplified if their gain is larger than their loss. The lasing threshold can be reached by tuning the driving field intensity and the medium length.

To start our analysis, we assume that  $\rho_{bb}$ ,  $\rho_{cc}$ , and  $\rho_{cb}$  evolve only under the influence of the driving field for the moment (see the corresponding equations in the Appendix) because the laser field coupled with  $a \leftrightarrow b$  transition is relatively weak. The drive field  $\Omega^{\text{drive}} = \Omega_d \cos[\nu_d(t - z/c)]$  is turned on adiabatically. We look for the solutions in the forms,

$$\rho_{bc}(t, z) = \sum_m \rho_{bc}^m e^{-im\nu_d(t-z/c)}, \quad (1)$$

$$\rho_{bb}(t, z) = \sum_m \rho_{bb}^m e^{-im\nu_d(t-z/c)}. \quad (2)$$

A set of infinite coupled algebraic equations can be derived and the solutions for  $\rho_{bc}^m$  and  $\rho_{bb}^m$  are found numerically. The detail is in the Appendix.

The propagation of the laser pulse is described by Maxwell's equation [8]

$$\left( c^2 \frac{\partial^2}{\partial z^2} - \frac{\partial^2}{\partial t^2} \right) \Omega^{\text{laser}} = \frac{2\Omega_a^2}{\omega_{ab}} \frac{\partial^2}{\partial t^2} (\rho_{ab} + c.c.), \quad (3)$$

where  $\Omega_a \equiv \sqrt{\frac{3N\lambda_{ab}^2\gamma c}{8\pi}}$ , where  $N$  is the density,  $\lambda_{ab}$  is the  $a \rightarrow b$  transition wavelength,  $\gamma$  is the  $a \rightarrow b$  radiative decay rate, and  $c$  is the speed of light. The atomic coherences  $\rho_{ab}$  and  $\rho_{ac}$  evolve with Eqs. (A-1) and (A-2) in the Appendix. We are looking for a solution in the

form of a superposition of spectral components without the rotating-wave-approximation (RWA) [19],

$$\Omega^{\text{laser}}(t, z) = \sum_m \Omega_l^m(z) e^{-i(\omega_{ab} + m\nu_d + \Delta\nu)(t-z/c)} + c.c., \quad (4)$$

$$\rho_{ab}(t, z) = \sum_m \rho_{ab}^m(z) e^{-i(\omega_{ab} + m\nu_d + \Delta\nu)(t-z/c)}, \quad (5)$$

$$\rho_{ac}(t, z) = \sum_m \rho_{ac}^m(z) e^{-i(\omega_{ab} + m\nu_d + \Delta\nu)(t-z/c)}, \quad (6)$$

where  $m = 0, \pm 1, \pm 2, \dots$ , and  $\Delta\nu$  is the small detuning of the lasing frequency from the frequency  $\omega_{ab} + m\nu_d$ . By using the expressions in Eqs. (4)-(6) and taking the components for the same frequency mode  $m$  with slowly-varying-envelope approximation (SVEA), the equations of the evolution of the laser field becomes

$$\frac{\partial}{\partial z} \Omega_l^m = i \frac{\omega_m}{\omega_{ab}} \frac{\Omega_a^2}{c} \rho_{ab}^m, \quad (7)$$

where  $\omega_m \equiv \omega_{ab} + m\nu_d + \Delta\nu$ . Here introduce next set of coupled algebraic equations which combines the equations that describe the evolution of the coherence  $\rho_{ab}$  and  $\rho_{ac}$

$$\Phi_m^- \rho_{ab}^{m-2} + \Phi_m^0 \rho_{ab}^m + \Phi_m^+ \rho_{ab}^{m+2} = - \sum_q \Theta_m^{2q} \Omega_l^{m-2q}, \quad (8)$$

where we define  $\eta_m^\pm \equiv 1/(\omega_{cb} \pm \nu_d + m\nu_d + \Delta\nu + i\gamma_t)$ , and

$$\Phi_m^\pm \equiv -\frac{\Omega_d^2}{4} \eta_m^\pm, \quad (9)$$

$$\Phi_m^0 \equiv (m\nu_d + \Delta\nu + i\gamma_t) - \frac{\Omega_d^2}{4} (\eta_m^- + \eta_m^+), \quad (10)$$

$$\Theta_m^{2q} \equiv \rho_{bb}^{2q} - \rho_{aa}(0) \delta_{q0} + \frac{\Omega_d}{2} (\eta_m^- \rho_{bc}^{2q-1} + \eta_m^+ \rho_{bc}^{2q+1}). \quad (11)$$

Eq. (8) indicates that the component of the field at the mode  $m$  is coupled with those at modes  $m \pm 2n$ , where  $n$  is the positive integer.

We search for a solution of Eq. (8) is searched in the form,

$$\Omega_l^m(z) = \sum_n u_n \varepsilon_n^m e^{ik_n z}. \quad (12)$$

Using this form in Eq. (7), we obtain

$$\rho_{ab}^m(z) = \frac{\omega_{ab}}{\omega_{ab} + m\nu_d + \Delta\nu} \frac{c}{\Omega_a^2} \sum_n u_n \varepsilon_n^m k_n e^{ik_n z}. \quad (13)$$

With the trial solutions of  $\Omega_l^m$  and  $\rho_{ab}^m$ , Eq. (8) results in a set of infinite linear equations with eigenvalues  $k_n$  and their corresponding eigenvectors  $\hat{\varepsilon}_n =$

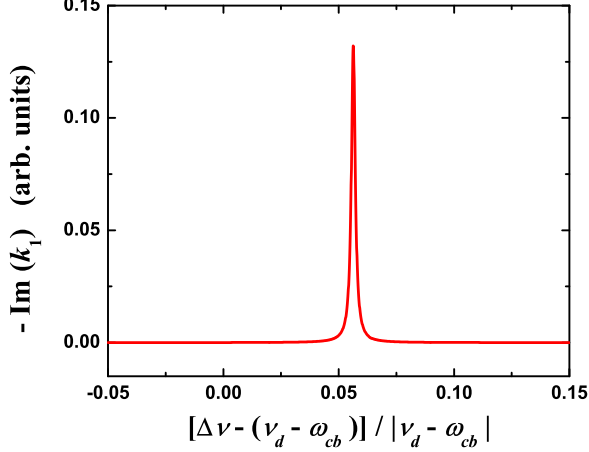


FIG. 2: (Color online) The imaginary part of  $k_1$  as a function of the lasing frequency detuning  $\Delta\nu$ . The populations are  $\rho_{aa}(0) = 0.1$ ,  $\rho_{bb}(0) = 0.9$  and  $\rho_{cc}(0) = 0$ , i.e., without inversion.  $\omega_{ab} = 5.0\omega_{cb}$ ,  $\Omega_a = 0.05\omega_{cb}$ ,  $\gamma_t = 10^{-4}\omega_{cb}$ . We drive the  $c \rightarrow b$  transition with a weak detuned field with  $\nu_d = 1.1\omega_{cb}$  and  $\Omega_d = 0.05\omega_{cb}$ . We cut off our calculation at  $m = \pm 10$ .

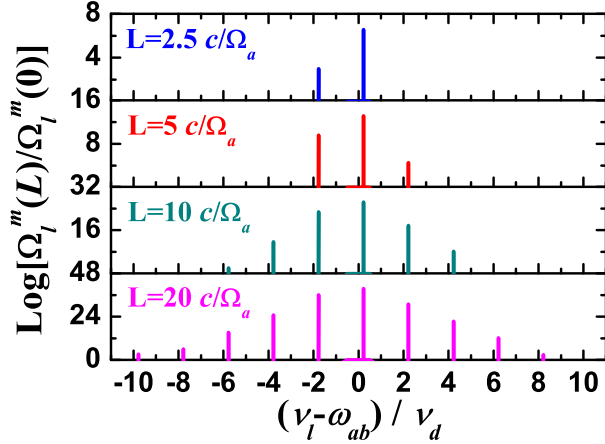


FIG. 3: (Color online) The amplification of the output field in the whole spectral gain region are plotted with different propagation lengths.

$(\dots, \varepsilon_n^{m-2}, \varepsilon_n^m, \varepsilon_n^{m+2}, \dots)^T$ . The coefficient  $u_n$  is determined by the boundary conditions for  $\Omega_l^m(z=0)$  and it reads  $u_n = \sum_m \varepsilon_n^m \Omega_l^m(z=0)$ . There are infinite frequency modes coupled in the system. However, the spectra must have a central spectral region where all the frequency modes have relatively strong intensities while the other frequencies far away from this region fade out gradually. Therefore, we can solve Eq. (8) numerically in a central spectral region where it has central mode  $m=0$  and boundary modes  $m=m_0$ . The set of infinite equations is truncated to dimension  $(m_0+1) \times (m_0+1)$  [20].

We first show the basic result in Fig. 2. The gain is characterized by the imaginary parts of eigenvalues  $k_n$  ( $n=1, 2, \dots$  with descending magnitudes of their imaginary parts) of Eq. (8), since the fields generally follow  $\sim e^{-\text{Im}(k_1)z}$ . Especially, we focus on the leading eigenvalue  $k_1$  whose imaginary part has a magnitude several orders larger than the rest. A peak of  $-\text{Im}(k_1)$  appears at  $\Delta\nu \sim 1.05\Delta$  with width  $\sim 0.01\Delta$  where  $\Delta \equiv \nu_d - \omega_{cb}$ . We therefore can observe sideband LWI in this region.

The amplitude of the output field at different frequency mode  $m$  ( $\Omega_l^m$ ) is determined by Eq. (12). The gain of each frequency component is not only dependent on the imaginary part of the eigenvalues, but also dependent on the coefficients such as  $\varepsilon_n^m$ , the elements in the eigenstates and  $u_n$  due to the boundary condition. It results in different lasing amplifications for different frequency modes. If the field component has smaller coefficients, it requires a longer propagation length to be amplified. The result is plotted in Fig. 3 for different propagation lengths. We find that we achieve amplification without inversion even for high-order frequency components. With longer propagation length, lasing for the higher-order modes gets amplified. In particular the laser fields at the blue-shifted sidebands ( $m > 0$ ) can provide a promising choice for generating a high-frequency coherent light source by a low-frequency drive field. For the field at mode  $m$  ( $\Omega_l^m(z)$ ) with frequency  $\sim \omega_{ab} + m\nu_d$ , the component of  $k_1$  in Eq. (12) does not dominate over the components of the other eigenvalues for small  $z$ , so the field component  $\Omega_l^m(z)$  is not get amplified compared to its initial value ( $\Omega_l^m(0)$ ). This means that laser field has threshold behavior and the one at a larger frequency mode has a higher threshold value (see Fig. 4). We see that the amplification quantity  $\log[\Omega_l^m(L)/\Omega_l^m(0)]$  is linearly dependent on the propagation length  $L$  only if the propagation length  $L$  exceeds the threshold value. In this regime, the linear coefficients for each curve at different frequency modes are the same because the leading terms in Eq. (12) for all modes  $m$  are the components of  $k_1$  for large  $z$  and all those terms grow according to  $\exp(-\text{Im}(k_1)z)$ .

The amplification of the laser pulse in the whole spectral region has a common source  $-\text{Im}(k_1)$ . We study the relation between  $k_1$  and the drive field Rabi frequency  $\Omega_d$  with all the other parameters fixed. We solve Eq. (8) numerically for various  $\Omega_d$  and search the maximum value of  $-\text{Im}(k_1)_{\text{max}}$ , by scanning the lasing frequency detuning  $\Delta\nu$  for each set of parameters. The dependence of the quantity  $-\text{Im}(k_1)_{\text{max}}$  with its corresponding lasing frequency detuning  $\Delta\nu$  on different  $\Omega_d$  are plotted in Fig. 5. All of the other parameters are the same as in Fig. 2. We find that the quantity  $-\text{Im}(k_1)_{\text{max}}$  is increasing with the drive field Rabi frequency  $\Omega_d$  when  $\Omega_d$  is small. Nevertheless  $-\text{Im}(k_1)_{\text{max}}$  has a maximum after which it drops counter-intuitively with increasing  $\Omega_d$ .

The simple but important physics behind the gain pro-

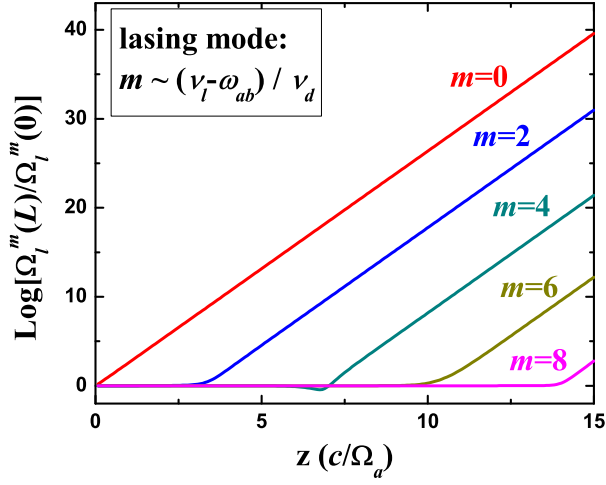


FIG. 4: (Color online) The gain of the output field for different modes  $m$  in the blue-shifted spectral region as a function of the propagation distances  $z$ .

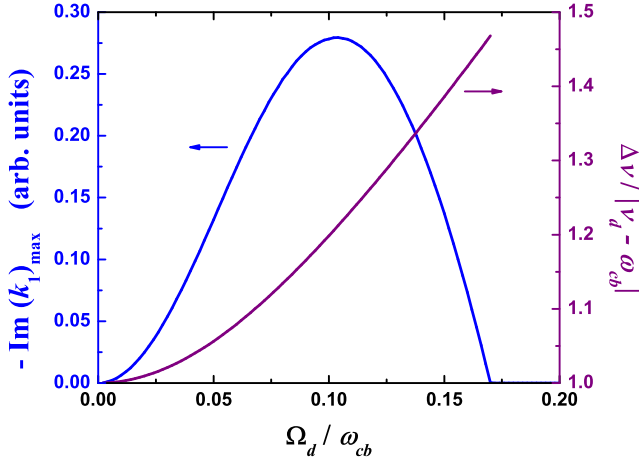


FIG. 5: (Color online) The maximum value of the negative imaginary part of the eigenvalue  $k_1$ ,  $-\text{Im}(k_1)_{\text{max}}$ , (left blue) with its corresponding lasing frequency detuning  $\Delta\nu$  (right purple) for various drive field Rabi frequency  $\Omega_d$ . The corresponding  $\Delta\nu$  is only plotted for positive  $-\text{Im}(k_1)$ .

file shown in Fig. 5 can be understood by considering the dressed state picture with only the 0<sup>th</sup>-order lasing transition. By driving the  $c \rightarrow b$  transition, the excited state  $a$  is coupled with two dressed states and both of the transition frequencies are on the order of  $\omega_{ab}$ . The energy difference of two dressed states depends on the drive field Rabi frequency  $\Omega_d$  and the drive field detuning  $\Delta$ . The initial population in the ground state  $b$  is redistributed to the two dressed states. While there is no population inversion in the bare-state system, it is still possible to achieve transient lasing because of the population inversion in dressed-state picture. If  $\Omega_d \rightarrow 0$ , one of the two

dressed states has  $\sim 0$  population, but the corresponding coupling strength between this dressed state and the excited state is also  $\rightarrow 0$ . Larger  $\Omega_d$  leads to the enhancement of this coupling strength and results in the increase of the gain or the quantity  $-\text{Im}(k_1)_{\text{max}}$ . However, the increase of  $\Omega_d$  also leads to more population in this dressed state, resulting in less population inversion. The competition between these two mechanisms is the reason that the quantity  $-\text{Im}(k_1)_{\text{max}}$  has the maximum positive value when  $\Omega_d$  is near the resonance  $\sim 0.1\omega_{cb}$  (see Fig. 5). Only one of the two dressed states can have less population than the excited state, so there is only one peak of the imaginary part of the eigenvalue  $k_1$  as shown in Fig. 2. (This is summarized in the detailed derivation in the Appendix.) Changing the drive field Rabi frequency also modifies the energies of the two dressed states, so the corresponding lasing frequency detuning  $\Delta\nu$  is increasing versus  $\Omega_d$  (right purple curve in Fig. 5).

Finally, we show the detailed numerical simulation with the full-set of Maxwell and Schrödinger equations including population evolutions without any approximation except SVEA in Fig. 6. We use the polarization source term in the equations to describe production rate of the dipole due to the spontaneous emission [23]. We see multiple single-pass gain peaks above the noise level and they are located at the lasing frequencies  $\nu_l^{\pm 2n} \sim \omega_{ab} \pm 2n\nu_d$ . There is no population inversion in the system. Coherent emission is generated directly from vacuum fluctuations without an initial seed pulse. The results of the amplification are generally linearly dependent on  $\Omega_a L$ . This feature gives us flexibility for choosing parameters in future experiments. For example, if the system has a smaller  $\Omega_a$  than what we propose, it can still produce the same amount of gain as what we expect by increasing  $L$ . Next, we propose a realistic experimental choice in a helium plasma gas which is partially excited to the metastable triplet state,  $2^3S_1$ , as realized in one recent experiment [11]. There we have the density  $\sim 10^{16} \text{ cm}^{-3}$  and we can drive the infrared transition  $2^3P_1 \rightarrow 2^3S_1$  (1083 nm) with a drive field wavelength as  $\lambda_d = 1022 \text{ nm}$  and a Rabi frequency of  $\Omega_d \sim 10^{14} \text{ rad/s}$ . Transient LWI occurs at the ultraviolet transition  $3^3P_1 \rightarrow 2^3S_1$  (388.9 nm). Then the high-order sideband generation of the coherent emission without any population inversion in the transient regime would have wavelengths as  $\lambda_l^{(2)} \sim 220.8 \text{ nm}$ ,  $\lambda_l^{(4)} \sim 154.2 \text{ nm}$ , etc. In a 1-cm long medium, we find a single-pass nano-Joule level coherent emission at the frequency  $\sim 220.8 \text{ nm}$  with the parameters listed above. The emitted pulse has a pulse width  $\sim 10 \text{ ps}$  such that the amplification is faster than any decay rate.

In conclusion, we study high-order sideband transient LWI in a V-scheme system. We use the Floquet method to solve the system in the weak lasing field limit (the population is unchanged due to the lasing field) and find

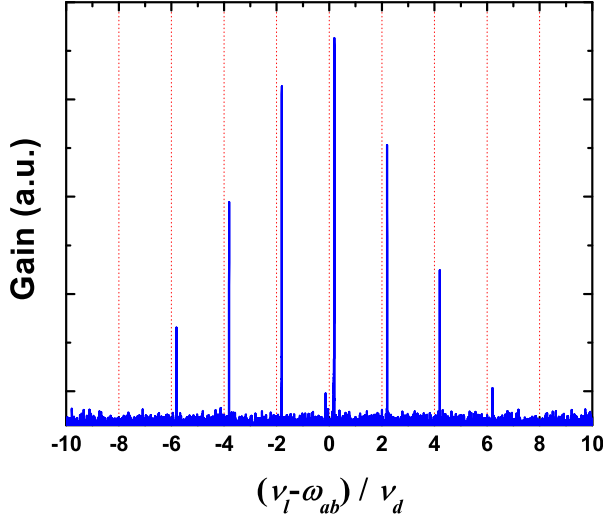


FIG. 6: (Color online) Detailed numerical experiments with parameters:  $\nu_d = 1.06\omega_{cb}$ ,  $\Omega_d = 0.18\omega_{cb}$ ,  $\Omega_a = 0.0754\omega_{cb}$ ,  $L = 7.54c/\Omega_a$ ,  $\rho_{aa}(0) = 0.15$ ,  $\rho_{bb}(0) = 0.85$ ,  $\rho_{cc}(0) = 0$ , and  $\gamma_t = 10^{-4}\omega_{cb}$ .

amplifications in different frequency modes. Threshold behaviour is seen for high-order sidebands. Amplification of the blue-shifted (higher-frequency) spectral region is interesting as a method for the generation of a coherent light source in the XUV or X-ray. Our simulation with experimental parameters shows coherent light emission at high frequency without population inversion. Furthermore, this method can potentially be extended to ultrashort pulse generation by attenuating the fields at different frequency modes to equal values with frequency-resolved filters. [19, 24, 25].

The authors thank C. O'Brien for useful discussion. We acknowledge the support of the National Science Foundation Grants PHY-1241032, PHY-1205868 and the Robert A. Welch Foundation (Awards A-1261). L.Y. is supported by the Herman F. Heep and Minnie Belle Heep Texas A&M University Endowed Fund held/administered by the Texas A&M Foundation.

#### Appendix A. Density matrix equations for a V-scheme model

Here we list the full-set of the density matrix equations for a V-scheme model shown in Fig. 1,

$$\dot{\rho}_{ab} = -(i\omega_{ab} + \gamma_t)\rho_{ab} + i\Omega^{\text{laser}}(\rho_{bb} - \rho_{aa}) - i\Omega^{\text{drive}}\rho_{ac}, \quad (\text{A-1})$$

$$\dot{\rho}_{ac} = -(i\omega_{ac} + \gamma_t)\rho_{ac} + i\Omega^{\text{laser}}\rho_{bc} - i\Omega^{\text{drive}*}\rho_{ab}, \quad (\text{A-2})$$

$$\dot{\rho}_{cb} = -(i\omega_{cb} + \gamma_t)\rho_{cb} + i\Omega^{\text{drive}}(\rho_{bb} - \rho_{cc}) - i\Omega^{\text{laser}}\rho_{ca}, \quad (\text{A-3})$$

$$\dot{\rho}_{bb} = -i\Omega^{\text{drive}}\rho_{bc} + i\Omega^{\text{drive}*}\rho_{cb} - i\Omega^{\text{laser}}\rho_{ba} + i\Omega^{\text{laser}*}\rho_{ab}, \quad (\text{A-4})$$

$$\dot{\rho}_{cc} = i\Omega^{\text{drive}}\rho_{bc} - i\Omega^{\text{drive}*}\rho_{cb}, \quad (\text{A-5})$$

$$\rho_{aa} + \rho_{bb} + \rho_{cc} = 1, \quad (\text{A-6})$$

where  $\gamma_t$  is the total decoherence rate. These equations are supplemented by Maxwell's equation

$$\left(\frac{\partial^2}{\partial z^2} - \frac{1}{c^2}\frac{\partial^2}{\partial t^2}\right)E^{\text{laser}} = \mu_0\frac{\partial^2 P^{\text{laser}}}{\partial t^2}, \quad (\text{A-7})$$

where  $P^{\text{laser}} = N(\wp_{ba}\rho_{ab} + c.c.)$ .

#### Appendix B. Floquet equations for the two-level system with a detuned drive field

Here we consider two-level system ( $c \rightarrow b$ ) with a detuned drive field  $\Omega^{\text{drive}} = \Omega_d \cos[\nu_d(t - z/c)]$  as shown in Fig. 1. We look for the solutions in the forms  $\rho_{bc}(t, z) = \sum_m \rho_{bc}^m e^{-im\nu_d(t-z/c)}$  and  $\rho_{bb}(t, z) = \sum_m \rho_{bb}^m e^{-im\nu_d(t-z/c)}$  for the equations,

$$\dot{\rho}_{bc} = (i\omega_{cb} - \gamma/2)\rho_{bc} - i\Omega^{\text{drive}}(\rho_{bb} - \rho_{cc}), \quad (\text{B-1})$$

$$\dot{\rho}_{bb} = \gamma\rho_{cc} - i\Omega^{\text{drive}}\rho_{bc} + i\Omega^{\text{drive}*}\rho_{cb}, \quad (\text{B-2})$$

$$\rho_{bb} + \rho_{cc} = \rho_{bb}(0) + \rho_{cc}(0), \quad (\text{B-3})$$

where the depopulation decay rate  $\gamma$  is a very small number and is present in order to avoid zero in the denominator. Therefore, the set of coupled algebraic equations are found to be

$$\begin{aligned} (m\nu_d + \omega_{cb} + i\gamma/2)\rho_{bc}^m - \Omega_d(\rho_{bb}^{m-1} + \rho_{bb}^{m+1}) \\ = -\frac{\Omega_d}{2}(\delta_{m,1} + \delta_{m,-1})[\rho_{bb}(0) + \rho_{cc}(0)], \end{aligned} \quad (\text{B-4})$$

$$\begin{aligned} (m\nu_d + i\gamma)\rho_{bb}^m - \frac{\Omega_d}{2}(\rho_{bc}^{m+1} + \rho_{bc}^{m-1} - \rho_{bc}^{-m+1*} - \rho_{bc}^{-m-1*}) \\ = i\gamma[\rho_{bb}(0) + \rho_{cc}(0)]\delta_{m,0}. \end{aligned} \quad (\text{B-5})$$

General results for  $\rho_{bc}^m$  and  $\rho_{bb}^m$  can be found by solving infinite coupled Eqs. (B-4) and (B-5) numerically. Note from Eq. (B-5) that  $\rho_{bb}^m = \rho_{bb}^{-m*}$ , which lead to the real solution for  $\rho_{bb}$ .



### Appendix C. LWI in the dressed state picture

Here we consider only the 0<sup>th</sup>-order lasing transition in the dressed state picture. The drive field couples the  $c \rightarrow b$  transition and has the form  $\Omega^{\text{drive}} = \Omega_d \cos(\nu_d \tau)$ , where  $\tau = t - z/c$ . With the rotating-wave-approximation, the interaction Hamiltonian is

$$V = -\hbar\Delta|c\rangle\langle c| - \frac{\hbar\Omega_d}{2}|c\rangle\langle b| - \frac{\hbar\Omega_d}{2}|b\rangle\langle c|, \quad (\text{C-1})$$

where  $\Delta = \nu_d - \omega_{cb}$ . It has two eigenstates as

$$|+\rangle = \sqrt{\frac{\Omega_{\text{eff}} - \Delta}{\Omega_{\text{eff}}}}|c\rangle - \sqrt{\frac{\Omega_d^2}{2\Omega_{\text{eff}}(\Omega_{\text{eff}} - \Delta)}}|b\rangle, \quad (\text{C-2})$$

$$|-\rangle = \sqrt{\frac{\Omega_{\text{eff}} + \Delta}{\Omega_{\text{eff}}}}|c\rangle + \sqrt{\frac{\Omega_d^2}{2\Omega_{\text{eff}}(\Omega_{\text{eff}} + \Delta)}}|b\rangle, \quad (\text{C-3})$$

where  $\Omega_{\text{eff}} \equiv \sqrt{\Omega_d^2 + \Delta^2}$  and their corresponding eigenvalues are

$$\omega_{\pm} = \frac{1}{2}(-\Delta \pm \Omega_{\text{eff}}). \quad (\text{C-4})$$

For a system which is initially at state  $|b\rangle$  at  $\tau = 0$ , the system evolves as

$$\begin{aligned} |\psi(\tau)\rangle = & -\sqrt{\frac{\Omega_{\text{eff}} + \Delta}{2\Omega_{\text{eff}}}}\sqrt{\rho_{bb}(0)}e^{-i\omega_+\tau}|+\rangle \\ & + \sqrt{\frac{\Omega_{\text{eff}} - \Delta}{2\Omega_{\text{eff}}}}\sqrt{\rho_{bb}(0)}e^{-i\omega_-\tau}|-\rangle \end{aligned} \quad (\text{C-5})$$

at  $\tau = t - z/c \geq 0$ . Therefore, the density matrix elements are

$$\rho_{++}(t, z) = \frac{\Omega_{\text{eff}} + \Delta}{2\Omega_{\text{eff}}}\rho_{bb}(0), \quad (\text{C-6})$$

$$\rho_{--}(t, z) = \frac{\Omega_{\text{eff}} - \Delta}{2\Omega_{\text{eff}}}\rho_{bb}(0), \quad (\text{C-7})$$

$$\rho_{+-}(t, z) = -\frac{\sqrt{\Omega_{\text{eff}}^2 - \Delta^2}}{2\Omega_{\text{eff}}}\rho_{bb}(0)e^{-i(\omega_+ - \omega_-)(t - z/c)}, \quad (\text{C-8})$$

$$\rho_{-+}(t, z) = -\frac{\sqrt{\Omega_{\text{eff}}^2 - \Delta^2}}{2\Omega_{\text{eff}}}\rho_{bb}(0)e^{i(\omega_+ - \omega_-)(t - z/c)}, \quad (\text{C-9})$$

Now, we introduce weak lasing field  $E_l$  with frequency  $\nu_l \sim \omega_{ab}$  coupling with the  $a \rightarrow b$  transition. The Hamiltonian reads

$$H = \omega_a|a\rangle\langle a| + \omega_+|+\rangle\langle +| + \omega_-|-\rangle\langle -|$$

$$- \wp_{ab}E_l e^{-i\nu_l t}|a\rangle\langle b| - \wp_{ba}E_l^* e^{i\nu_l t}|b\rangle\langle a|$$

$$= \omega_a|a\rangle\langle a| + \omega_+|+\rangle\langle +| + \omega_-|-\rangle\langle -|$$

$$+ (-\wp_{a+}E_l e^{-i\nu_l t}|a\rangle\langle +| - \wp_{a-}E_l e^{-i\nu_l t}|b\rangle\langle -| + H.c.), \quad (\text{C-10})$$

where

$$\wp_{a+} \equiv -\sqrt{\frac{\Omega_{\text{eff}} + \Delta}{2\Omega_{\text{eff}}}}\wp_{ab}, \quad (\text{C-11})$$

$$\wp_{a-} \equiv \sqrt{\frac{\Omega_{\text{eff}} - \Delta}{2\Omega_{\text{eff}}}}\wp_{ab}. \quad (\text{C-12})$$

We assume that  $E_l$  is so weak that it doesn't change the populations and the coherence between states  $|+\rangle$  and  $|-\rangle$ . Therefore we find

$$\frac{d}{dt}\tilde{\rho}_{a+} = -i(\omega_{a+} - \nu_l)\tilde{\rho}_{a+}$$

$$-i\wp_{a+}E_l[\rho_{aa}(0) - \rho_{++}] + i\wp_{a-}E_l\rho_{-+}, \quad (\text{C-13})$$

$$\frac{d}{dt}\tilde{\rho}_{a-} = -i(\omega_{a-} - \nu_l)\tilde{\rho}_{a-}$$

$$-i\wp_{a-}E_l[\rho_{aa}(0) - \rho_{--}] + i\wp_{a+}E_l\rho_{+-}, \quad (\text{C-14})$$

where  $\omega_{a\pm} \equiv \omega_a - \omega_{\pm}$ , and  $\tilde{\rho}_{a\pm} \equiv \rho_{a\pm}e^{i\nu_l t}$ . The Maxwell's equation has the expression

$$\left(\frac{\partial}{\partial t} + c\frac{\partial}{\partial z}\right)E_l = \frac{i\nu_l}{2\epsilon_0}\wp_{ab}\tilde{\rho}_{ab} = \frac{i\nu_l}{2\epsilon_0}(\wp_{a+}\tilde{\rho}_{a+} + \wp_{a-}\tilde{\rho}_{a-}). \quad (\text{C-15})$$

If we take RWA and neglect all the fast-oscillating terms, then  $E_l$  is only possible to get amplified at the resonant frequency  $\nu_l^{\pm} = \omega_{a\pm}$  with the corresponding coherence as

$$\frac{d}{dt}\tilde{\rho}_{a\pm} = -i\wp_{a\pm}E_l\left[\rho_{aa}(0) - \frac{\Omega_{\text{eff}} \pm \Delta}{2\Omega_{\text{eff}}}\rho_{bb}(0)\right]. \quad (\text{C-16})$$

Hence the electrical field  $E_l$  evolves as

$$\begin{aligned} & \left(\frac{\partial}{\partial t} + c\frac{\partial}{\partial z}\right)\dot{E}_l \\ &= \frac{\nu_l\wp_{ab}^2}{2\epsilon_0}\left\{\frac{\Omega_{\text{eff}} \pm \Delta}{2\Omega_{\text{eff}}}\left[\rho_{aa}(0) - \frac{\Omega_{\text{eff}} \pm \Delta}{2\Omega_{\text{eff}}}\rho_{bb}(0)\right]\right\}E_l. \end{aligned} \quad (\text{C-17})$$

From this result, we find that the electrical field  $E_l$  can get amplified if there is population inversion between state  $|a\rangle$  and state  $|\pm\rangle$  in the dressed state picture. We consider the case that  $\rho_{aa}(0) \ll \rho_{bb}(0)$  and assume  $\Delta > 0$ . Lasing happens at the transition between the

state  $|a\rangle$  and the state  $|-\rangle$  and gain is dependent on the quantity  $\frac{\Omega_{\text{eff}} - \Delta}{2\Omega_{\text{eff}}} \left[ \rho_{aa}(0) - \frac{\Omega_{\text{eff}} - \Delta}{2\Omega_{\text{eff}}} \rho_{bb}(0) \right]$ . When  $\Omega_d \rightarrow 0$ , gain  $\rightarrow 0$  since  $\frac{\Omega_{\text{eff}} - \Delta}{2\Omega_{\text{eff}}} \rightarrow 0$  though there is population inversion  $\rho_{aa}(0) > \frac{\Omega_{\text{eff}} - \Delta}{2\Omega_{\text{eff}}} \rho_{bb}(0)$ . Gain is increasing with the increase of  $\Omega_d$  initially. When it reaches the maximum value, it will decrease until it becomes zero when there is no population inversion  $\rho_{aa}(0) \leq \frac{\Omega_{\text{eff}} - \Delta}{2\Omega_{\text{eff}}} \rho_{bb}(0)$  for a very large  $\Omega_d$ . The corresponding lasing frequency is  $\nu_l = \omega_{a-} = \omega_{ab} + \frac{1}{2}(\Delta + \Omega_{\text{eff}})$ , which is increasing with  $\Omega_d$ . It has the similar result for the case  $\Delta < 0$  and the lasing happens at the transition between the state  $|a\rangle$  and the state  $|+\rangle$ .

- 
- [1] O.A. Kocharovskaya and Ya.I. Khanin, *JETP Lett.* **48**, 630 (1988).  
[2] S.E. Harris, *Phys. Rev. Lett.* **62**, 1033 (1989).  
[3] M.O. Scully, S.-Y. Zhu, and A. Gavrielides, *Phys. Rev. Lett.* **62**, 2813 (1989).  
[4] A.A. Svidzinsky, L. Yuan, and M.O. Scully, *New J. Phys.* **15**, 053044 (2013).  
[5] E.S. Fry, X. Li, D. Nikonov, G.G. Padmabandu, M.O. Scully, A.V. Smith, F.K. Tittel, C. Wang, S.R. Wilkinson, and S.-Y. Zhu, *Phys. Rev. Lett.* **70**, 3235 (1993).  
[6] M. Marthaler, Y. Utsumi, D.S. Golubev, A. Shnirman, and G. Schön, *Phys. Rev. Lett.* **107**, 093901 (2011).  
[7] M.F. Pereira, Jr. *Phys. Rev. B* **78**, 245305 (2008).  
[8] M.O. Scully and M.S. Zubairy, *Quantum Optics* (Cambridge University Press, New York, NY 1997).  
[9] A. Imamoglu, J. E. Field, and S. E. Harris, *Phys. Rev. Lett.* **66**, 1154 (1991).  
[10] S. Suckewer and P. Jaeglé, *Laser Phys. Lett.* **6**, 411 (2009).  
[11] H. Xia, A.A. Svidzinsky, L. Yuan, C. Lu, S. Suckewer, and M.O. Scully, *Phys. Rev. Lett.* **109**, 093604 (2012).  
[12] P. Cavalié, J. Freeman, K. Maussang, E. Strupiechonski, G. Xu, R. Colombelli, L. Li, A.G. Davies, E.H. Linfield, J. Tignon, and S.S. Dhillon, *Appl. Phys. Lett.* **102**, 221101 (2013).  
[13] H. Xiong, L.-G. Si, X.-Y. Lü, X. Yang, and Y. Wu, *Opt. Lett.* **38**, 353 (2013).  
[14] A.A. Lanin, I.V. Fedotov, V.I. Sokolov, A.B. Fedotov, A.S. Akhmanov, V.Ya. Panchenko, and A.M. Zheltikov, *Opt. Lett.* **35**, 3976 (2010).  
[15] A. Schliesser, R. Rivière, G. Anetsberger, O. Arcizet, and T.J. Kippenberg, *Nat. Phys.* **4**, 415 (2008).  
[16] S.N. Soda, S. Sensarn, M.Y. Shverdin, and G.Y. Yin, *Appl. Phys. Lett.* **91**, 241101 (2007).  
[17] A.E. Siegman, *lasers* (University Science Books, Sausalito, CA 1986).  
[18] A.A. Svidzinsky, L. Yuan, and M.O. Scully, *Phys. Rev. X* **3**, 041001 (2013).  
[19] Y.V. Radeonychev, V.A. Polovinkin, and O. Kocharovskaya, *Phys. Rev. Lett.* **105**, 183902 (2010).  
[20] A. Picón, L. Roso, J. Mompart, O. Varella, V. Ahufinger, R. Corbalán, and L. Plaja, *Phys. Rev. A* **81**, 033420 (2010).  
[21] G.N. Gibson, *Phys. Rev. Lett.* **89**, 263001 (2002).  
[22] D.-w. Wang, A.-j. Li, L.-g. Wang, S.-y. Zhu, and M.S. Zubairy, *Phys. Rev. A* **80**, 063826 (2009).  
[23] J.C. MacGillivray and M.S. Feld, *Phys. Rev. A* **14**, 1169 (1976).  
[24] S.E. Harris and A.V. Sokolov, *Phys. Rev. Lett.* **81**, 2894 (1998).  
[25] M. Zhi, K. Wang, X. Hua, and A.V. Sokolov, *Opt. Lett.* **36**, 4032 (2011).